International Journal Of Health Medicine and Current Research
E - ISSN : 2528 - 3189
P - ISSN : 2528 - 4398

International Journal of Health Medicine and Current Research
Vol. 4, Issue 03, pp.1362-1370, September, 2019

DOI:
10.22301/IJHMCR.2528-3189.1362

Article can be accessed online on:
http://www.ijhmcr.com

ORIGINAL ARTICLE

INTERNATIONAL JOURNAL OF HEALTH MEDICINE AND CURRENT RESEARCH

LAND SURFACE TEMPERATURE TREND IN SUMATRA ISLAND, INDONESIA: 2000-2018

Tofan Agung Eka Prasetya[1,2 *], Sarawuth Chesoh[1], Apiradee Lim[1], Donald Roy McNeil[1]

[1]Research Methodology, Departement of Mathematics and Computer Science, Faculty of Science and Technology, Prince of Songkla University, Pattani Campus, Muang, Pattani, 94000 THAILAND.
[2]Health Departement, Vocational Faculty, Universitas Airlangga, Jl. Dharmawangsa Dalam Selatan No 68, Airlangga, Gubeng, Surabaya, East Java, INDONESIA.

ARTICLE INFO

Article History:
Received 19th Jun, 2019
Received in revised form
20th Jul, 2019
Accepted 23th Aug, 2019
Published online 30th Sep, 2019

Key words:
Land Surface Temperature; Environment, Sumatra; Cubic Spline.

Correspondence to Author:
Tofan Agung Eka Prasetya
Health Departement, Vocational Faculty, Universitas Airlangga, Jl. Dharmawangsa Dalam Selatan No 68, Airlangga, Gubeng, Surabaya, East Java, INDONESIA.

E-mail:
tofank3@gmail.com

ABSTRACT

Land surface temperature (LST) is one of the important factors in the physics of land surface processes to ensure about temperature change in environment. Sumatra was one of the biggest islands in Indonesia that suffering from deforestation. The objective of this study was to investigate LST trend in Sumatra Island from 2000-2018. LST-day data for each super region of Sumatra island was analyze with cubic spline to see seasonal pattern. Daily seasonal pattern for LST-day (˚C) was not so many variations. The highest LST-day in all area of region 25 super region 1 happened between day 229 and day 267. LST-day was increased in the beginning of year and decreased at the end of the year. The other findings indicate that on a decade 28.2% of all Sumatera surface had been increasing, 35.6% decreasing, 36.3% stable.

Citation: Tofan Agung Eka Prasetya[1,2 *], Sarawuth Chesoh[1], Apiradee Lim[1], Donald Roy McNeil[1], 2019 "*Land Surface Temperature Trend In Sumatra Island, Indonesia: 2000-2018*", *International Journal of Health Medicine and Current Research*, 4, (03), 1362-1370.

INTRODUCTION

Climate change, particularly rising temperature, is one of the important environmental problem facing the world today. Satellite-based climate-related data, such as Land Surface Temperature (LST), play a critical role in monitoring climatological processes, land surface energy interactions and water balance at regional to global scales (1,2), as well as climate change impacts. These changes in climate affect human lives and have a large impact on society as a whole (3).

This is reflected in the slowing down of the long-term reduction in the prevalence of undernutrition, which is partly due to extreme climatic events (4).

This is particularly relevant for Southeast Asia because agriculture and food security are vulnerable sectors already and Southeast Asia has vital role as major exporter (5). Since the 1950s, the tropics have become a domain of permanently increasing interest among meteorologists mainly because the weather in the tropics is dominated by convective storms. These develop mainly along the Intertropical Convergence Zone (6).

A report finding claimed that Sumatra islands are chosen as research area because of high rates of deforestation (7). Sumatra Islands are also the largest of three islands that suffered from deforestation in Indonesia. Sumatra forest conversion into non-forest area has attracted national and international researchers. This study was investigated Land Surface Temperature trend in Sumatra Island. Thus, cubic splines as a statistical tool will be applied to investigate the seasonal pattern and time series trend of Land Surface Temperature in Sumatra. Cubic splines are very accurate in practice and the error depends on the second derivative(8). Multiple linear regression will be applied to analyze the correlation of elevation, land cover, and NDVI to Land Surface Temperature in Sumatra Island.

METHODS

This research uses secondary MODIS data which is obtained from NASA website where we focus on from 2000-2018. The data consist of LST and we concentrate on Sumatera Island, Indonesia. Moreover, we mainly have stand-points in seasonal pattern of LST. Time series trends and patterns of land surface temperature will be analyzed using cubic spline.

1.1. Study area

This study was conducted in Sumatra Islands. Sumatra archipelago includes the islands of Sumatra and small islands in vicinity. Sumatra islands located from east longitude 950 to 109.20 east longitude and north latitude 60 to 6,20 south latitude (Figure 1).

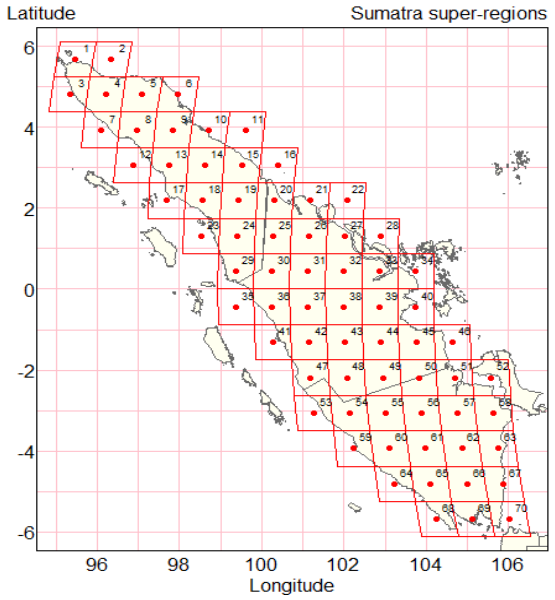

Figure 1. Super regions of Sumatra with the center of latitude and longitude.

This research attempt to analyze satellite data that might have several uncommon terminologies. Before going to further explanation about data source and data management, these are several terms used in this research to ensure readers have same view.

a. *Super region* is an area cover 105 km x 105 km using a specific coordinate latitude and longitude as central point. Sumatera Island consists of 70 super region and each of them covers 25 region.
b. *Region* is an area with large 21 km x 21 km and this area comprises 9 sub-region.
c. *Sub-region* is an area with dimension 7 km x 7 km which is contained 49 pixel with area 1 km x 1 km.
d. *Pixel* is our research unit which is compressed all satellite data (LST, LV, LC, and NDVI) in time series record from 2000-2018.

1.2. Data source

Land Surface Temperature data was data from independent data sets of Moderate Resolution Imaging Spectroradiometer (MODIS)(9–11). To get data from https://modis.ornl.gov we must sign in and decide the location centered on Latitude, Longitude which is calculated or converted by Modland tile calculator tool (https://landweb.modaps.eosdis.nasa.gov/cgi-bin/developer/tilemap.cgi) in vertical tile, horizontal tile, line, sample and put it in the website.

The analysis was only for land because the data was from MOD11A2 Terra Land Surface Temperature data(12). The analysis of this study was conducted with R program (13). The website will give the resume of

data that we download, and choose order, so the data set link will send to our email. LST and NDVI data must be ordered in different time, because the website only give one option name of data each order.

We must download LST data in CSV format and process extracting then raster each data that has been downloaded. The last step is processing and analyzed the data with R program (10,11). Land Surface Temperature data are independent set of data that can be freely downloaded from Moderate Resolution Imaging Spectroradiometer (MODIS) and https://earthexplorer.usgs.gov/. LST data are from MODIS 8 days Tera LST (MOD11A2) from 2000 to 2018 at 0.05° spatial resolution. The original LST degree measurement was Kelvin then converted into Celsius. MODIS 8 day LST data are mean of the clear-sky condition data only, and elevation data was extracted from LST data (9–11).

MODIS LST data were collected over time, they fluctuate over the season (1). The seasonal pattern was assumed to be the same for every year, and the change in other parameters such as the land cover change that has a direct or indirect effect on the LST data is consistently increasing or decreasing. A sudden natural disaster, for instance a forest fire or landslide or tsunami that could cause the instantaneous change of data behavior, is excluded in this model consideration. Ideally, the model should provide continuous seasonal patterns for each day of the year within a year. These considerations suggest that the most appropriate model is a cubic spline with specific boundary conditions that ensure smooth periodicity. Choosing the location and number of parameter knots for smoothing the spline curve is a critical issue. However, there are current strategies for the optimal selection of those parameters based on procedures to add knots in intervals where the residuals show trends as indicated by autocorrelation or in intervals where the residuals are inadmissibly significant (14).

RESULTS

Firstly, the R program was run for each super region to analyze LST day data with cubic spline and linear regression. Figure 2 and 3 show daily and annually LST for region 25 in super region 1 where both figures depicted distribution of records. Figure 4 show the LST change result for 25 regions in super region 1. After analyzing for 70 super regions, the result of p value and r-square was tabulated in Table 1.

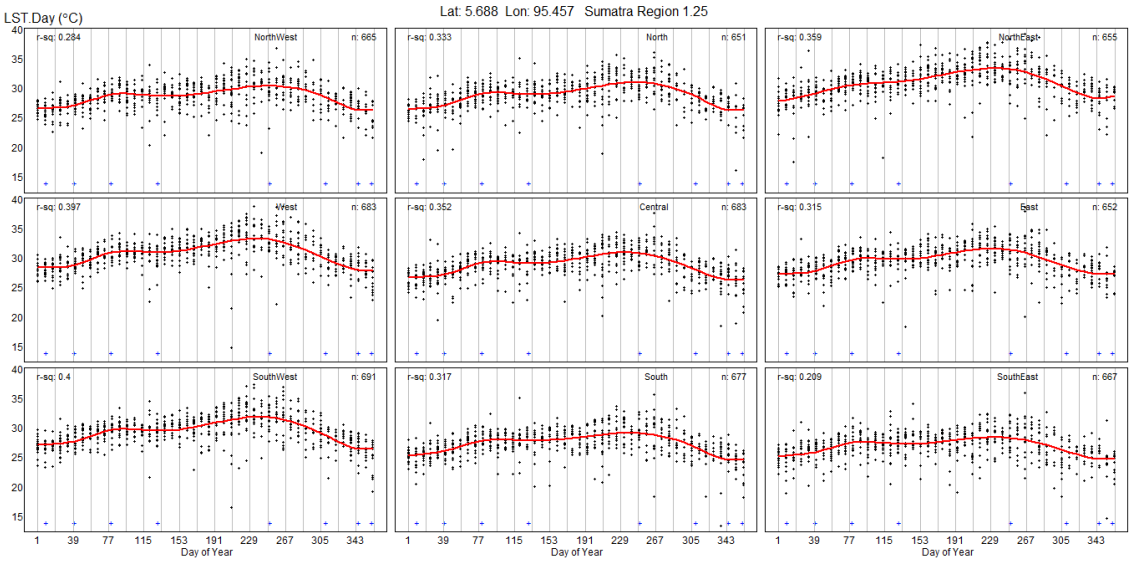

Figure 2. Daily LST – Day (°C) in Sumatra 2000-2018 Super Region 1, region 25.

Figure 2 visualized the distribution of daily record in 19 years that meant every scale in x-axis had 19 dots representing each year (if there is no missing value on it). According to Figure 2, daily seasonal pattern for LST-day (°C) was not so many variations. The highest LST-day in all area of region 25 super region 1 happened between day 229 and day 267. LST-day was increased in the beginning of year and decreased at the end of the year.

Figure 3 consisted of nine plots where each plot representing one center of region and eight point of compass (northwest, west, southwest, north, south, northeast, east, and southeast). According to Figure 3, LST increase per decade by cubic spline will show by red dot line and linear show by blue dot line. Figure 3

also showed the outlier value with the purple dot. Figure 3 depict that south (S), east (E), center (C) and south east (SE) area of super region 1 was area that predicted increased of LST. The other point area of super region 1 was predicted decreased.

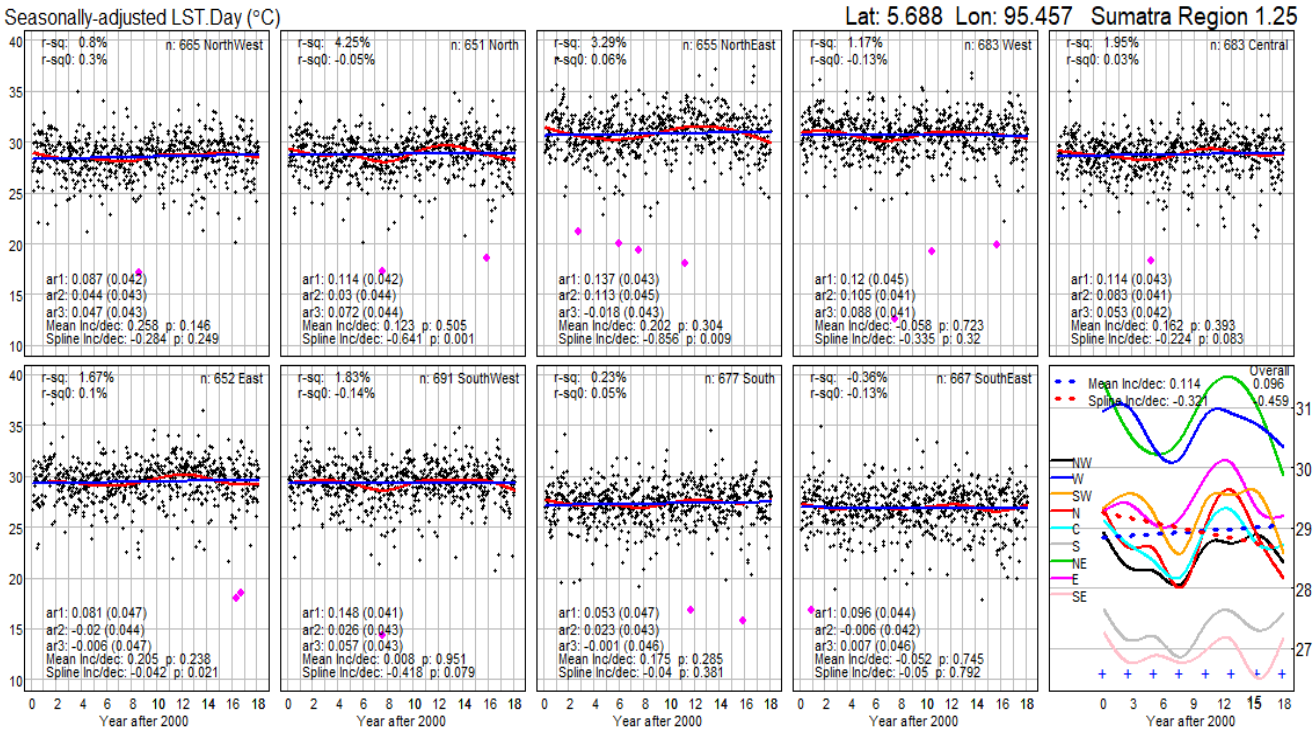

Figure 3. Seasonally-adjusted LST – day (°C) in Sumatra 2000-2018.

AR (ARIMA coefficient) 1 to 3 also shown in this figure and its mean that the program already take out the autocorrelation of LST-day data(15,16). Overall p-value and r squared had been released from the Figure 4. The increasing LST-day trend result for super region 1 was plot and show below. Figure 4 illustrated the change of LST in super region 1. It showed that in a decade this area was getting cooler where the spline indicated minus value.

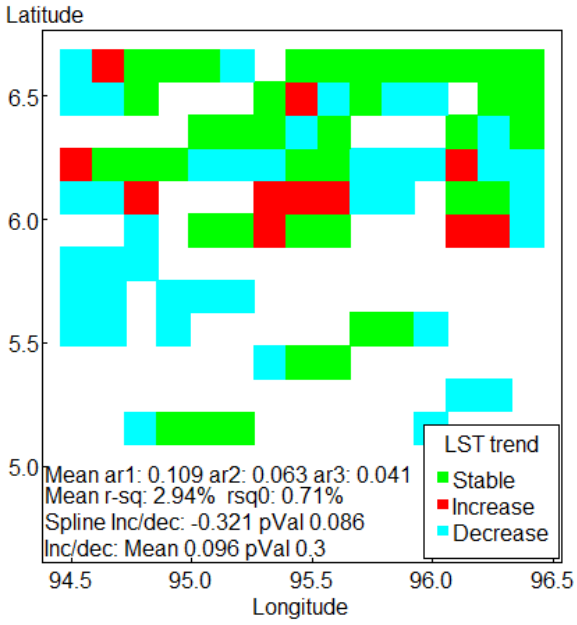

Figure 4. Plot of LST-day trend for super region 1.

As needed to gain best model and the highest r-square we run the program of cubic spline strat from 4 knots until 9 knots for 70 super regions of Sumatra. Based on the program and result, the cubic spline with 8 knots gives the highest r-square (for super region 1)-shown in Table 1. The highest r-square will be the criteria for deciding the best model also.

Table 1. Average p-value, r-square and knot by cubic spline for Sumatra super region 2000-2018.

	4 knots		5 knots		6 knots		7 knots		8 knots		9 knots	
	avg. R^2	avg. p-value	avg. R^2	avg. p-value	avg. R^2	avg. p-value	avg. R^2	avg. p-value	avg. R^2	avg. p-value	avg. R^2	avg. p-value
1	2.40	0.07	2.70	0.06	2.73	0.07	2.75	0.09	2.94	0.09	2.87	0.10
2	5.32	0.03	5.50	0.05	5.52	0.05	5.45	0.07	5.44	0.07	5.37	0.11
3	1.65	0.10	2.32	0.06	2.40	0.07	2.40	0.08	2.35	0.10	2.42	0.11
4	1.78	0.16	2.16	0.14	2.27	0.13	2.42	0.11	2.41	0.13	2.42	0.15
5	1.93	0.13	2.20	0.12	2.38	0.12	2.55	0.11	2.60	0.12	2.55	0.14
6	3.02	0.11	3.92	0.06	4.23	0.06	4.42	0.06	4.44	0.06	4.37	0.07
7	5.33	0.06	5.82	0.05	5.87	0.06	5.88	0.06	5.88	0.06	5.95	0.06
8	1.72	0.15	2.35	0.08	2.46	0.09	2.60	0.09	2.64	0.09	2.60	0.11
9	1.51	0.16	2.70	0.04	2.89	0.04	3.15	0.03	3.31	0.03	3.37	0.03
10	2.81	0.17	3.22	0.13	3.37	0.12	3.65	0.11	3.79	0.11	3.69	0.12
11	2.82	0.01	2.69	0.02	2.60	0.03	3.45	0.01	3.28	0.02	3.08	0.03
12	0.88	0.21	2.15	0.01	2.13	0.02	2.09	0.03	2.09	0.04	2.13	0.04
13	2.01	0.13	2.59	0.05	2.79	0.05	3.25	0.04	3.40	0.04	3.34	0.05
14	1.59	0.12	1.91	0.09	2.10	0.08	2.26	0.06	2.47	0.06	2.40	0.07
15	3.62	0.09	4.11	0.06	4.60	0.04	4.78	0.04	4.88	0.05	4.87	0.06
16	1.43	0.19	2.45	0.11	2.69	0.10	2.82	0.10	2.77	0.12	2.71	0.14
17	4.96	0.08	6.00	0.01	6.05	0.01	6.10	0.02	6.14	0.02	6.20	0.02
18	2.16	0.18	2.58	0.11	2.78	0.09	3.19	0.06	3.41	0.06	3.46	0.07
19	1.34	0.12	1.67	0.10	1.91	0.09	2.03	0.08	2.13	0.08	2.05	0.10
20	8.05	0.10	8.54	0.09	8.83	0.09	9.29	0.09	9.46	0.07	9.29	0.10
21	7.16	0.08	8.52	0.03	8.75	0.03	9.35	0.03	9.62	0.03	9.71	0.04
22	4.46	0.04	7.34	0.01	7.67	0.01	7.87	0.01	8.45	0.01	8.19	0.01
23	6.75	0.04	8.37	0.03	8.56	0.03	8.73	0.02	8.79	0.03	8.91	0.03
24	3.49	0.20	3.72	0.17	3.86	0.16	4.14	0.15	4.27	0.14	4.18	0.17
25	10.7	0.03	11.2	0.03	11.5	0.02	12.0	0.02	12.5	0.03	12.5	0.03
26	14.8	0.05	16.2	0.02	16.9	0.02	17.4	0.02	18.0	0.01	18.0	0.01
27	6.85	0.08	9.25	0.03	10.4	0.02	11.5	0.02	12.2	0.02	12.6	0.02
28	1.53	0.16	2.25	0.12	2.37	0.13	2.68	0.11	2.95	0.10	2.90	0.11
29	3.15	0.11	3.44	0.08	3.59	0.07	3.69	0.06	3.72	0.06	3.89	0.07
30	2.01	0.13	2.25	0.12	2.35	0.12	2.46	0.12	2.40	0.14	2.46	0.14
31	4.87	0.06	5.27	0.07	5.68	0.06	6.08	0.06	6.47	0.07	6.52	0.08
32	6.49	0.10	7.06	0.10	7.54	0.09	8.15	0.07	9.07	0.06	10.0	0.05
33	4.10	0.12	4.94	0.08	5.41	0.08	6.12	0.07	6.62	0.06	6.89	0.07
34	2.13	0.20	2.79	0.12	3.04	0.13	3.22	0.13	3.46	0.12	3.43	0.13
35	6.59	0.00	7.16	0.00	7.48	0.00	7.46	0.00	7.50	0.00	7.50	0.00

	4 knots		5 knots		6 knots		7 knots		8 knots		9 knots	
	avg. R^2	avg. p-value	avg. R^2	avg. p-value	avg. R^2	avg. p-value	avg. R^2	avg. p-value	avg. R^2	avg. p-value	avg. R^2	avg. p-value
36	1.82	0.14	2.13	0.12	2.32	0.11	2.43	0.11	2.43	0.12	2.41	0.14
37	3.58	0.11	3.80	0.11	4.18	0.12	4.33	0.12	4.46	0.12	4.62	0.11
38	12.9	0.02	13.7	0.02	14.1	0.03	14.5	0.03	14.7	0.03	15.0	0.03
39	7.45	0.05	7.72	0.06	8.11	0.06	8.19	0.07	8.49	0.06	8.67	0.07
40	1.53	0.15	1.88	0.13	1.92	0.14	1.95	0.14	2.07	0.14	1.99	0.16
41	2.68	0.05	3.14	0.05	3.28	0.05	3.47	0.05	3.66	0.04	3.76	0.04
42	2.56	0.13	2.77	0.13	2.86	0.14	3.09	0.13	3.09	0.13	3.15	0.15
43	9.11	0.03	9.42	0.04	9.78	0.04	9.78	0.05	9.78	0.05	9.88	0.06
44	7.33	0.04	7.64	0.04	7.92	0.04	8.71	0.03	9.05	0.04	9.53	0.04
45	2.59	0.21	3.73	0.13	3.88	0.13	3.91	0.15	4.13	0.16	4.21	0.18
46	1.50	0.14	1.67	0.14	1.73	0.15	2.03	0.13	2.39	0.10	2.54	0.10
47	5.18	0.10	5.44	0.11	5.53	0.12	5.65	0.12	5.75	0.12	5.89	0.11
48	3.71	0.03	3.76	0.04	3.79	0.04	3.84	0.05	3.88	0.06	3.85	0.06
49	7.16	0.03	7.35	0.03	7.65	0.03	7.70	0.03	7.70	0.04	7.76	0.04
50	7.95	0.06	8.47	0.06	8.94	0.06	9.19	0.07	9.50	0.07	9.70	0.08
51	4.04	0.13	4.45	0.13	4.62	0.13	4.87	0.13	4.99	0.13	5.00	0.13
52	3.48	0.10	4.32	0.05	4.92	0.04	5.59	0.03	5.78	0.04	5.85	0.05
53	3.95	0.04	4.15	0.03	4.51	0.03	4.61	0.03	4.53	0.04	4.62	0.04
54	2.22	0.06	2.40	0.07	2.45	0.08	2.66	0.07	2.79	0.07	2.83	0.08
55	3.47	0.05	3.68	0.06	3.99	0.05	4.22	0.05	4.40	0.05	4.45	0.05
56	5.50	0.08	5.96	0.08	6.18	0.08	6.38	0.08	6.54	0.09	6.65	0.10
57	4.52	0.25	5.00	0.21	5.32	0.20	5.56	0.20	5.85	0.20	6.21	0.19
58	2.97	0.30	3.61	0.25	5.61	0.19	6.64	0.15	7.84	0.12	8.55	0.11
59	3.68	0.02	5.49	0.01	5.72	0.01	5.94	0.01	6.03	0.01	6.07	0.01
60	3.27	0.07	3.61	0.07	3.75	0.06	4.01	0.05	4.18	0.05	4.47	0.05
61	5.64	0.06	5.98	0.07	6.88	0.05	7.32	0.04	7.94	0.04	8.79	0.02
62	8.71	0.13	9.11	0.13	9.56	0.13	9.76	0.14	10.1	0.15	10.4	0.13
63	3.73	0.21	4.71	0.14	5.45	0.13	5.87	0.13	6.22	0.13	6.47	0.14
64	2.80	0.05	3.82	0.02	4.05	0.02	4.24	0.02	4.22	0.02	4.29	0.03
65	4.54	0.07	4.96	0.05	5.83	0.03	6.16	0.03	6.36	0.04	6.64	0.04
66	3.46	0.28	3.76	0.27	4.28	0.25	4.44	0.29	4.68	0.31	5.18	0.29
67	1.45	0.44	2.40	0.29	2.68	0.30	2.74	0.34	2.79	0.39	3.37	0.34
68	2.53	0.07	3.56	0.03	3.96	0.02	4.86	0.01	5.23	0.01	5.42	0.01
69	1.98	0.19	2.18	0.21	2.53	0.16	2.50	0.20	2.75	0.21	3.30	0.16
70	3.08	0.23	3.29	0.27	3.66	0.25	3.74	0.28	4.03	0.29	4.33	0.29

The highest r-square per super region is obtained from cubic spline analysis as shown in Table 1 and for each super region possibly depict different results on knots. There are 3 considered criteria for analyzing overall model which were knots (17), p-value and r-square(18,19). The lowest knot, the lowest p-value, and the highest r-square will be selected to plot in map as shown in Figure 6. The changing of LST in °C/Decade with cubic spline will be shown as follows.

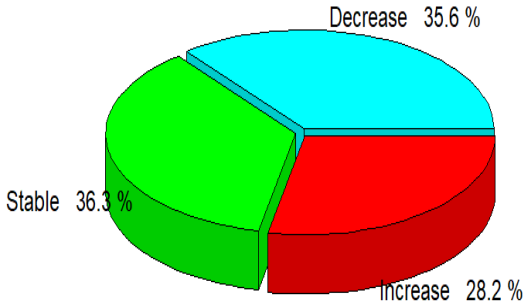

Figure 5. Percentage of LST-day changing by cubic spline model in Sumatra 2000-2018.

According to cubic spline result, the proportion of LST changing depicted as shown in figure 5 where more 28.2% of all Sumatera surface had been increasing on a decade. Decreasing of LST changing reach 35.6% of all Sumatra area which is higher ratio rather than increasing area. And 36.3% of all Sumatra area categorized stable LST changing. Figure 5 indicated that more than 1/3 part of Sumatera had decreased in a decade. Difference findings was shown in area of part Sumatra that in a decade, minimum air temperature showed significance increasing trend in North Sumatra (20).

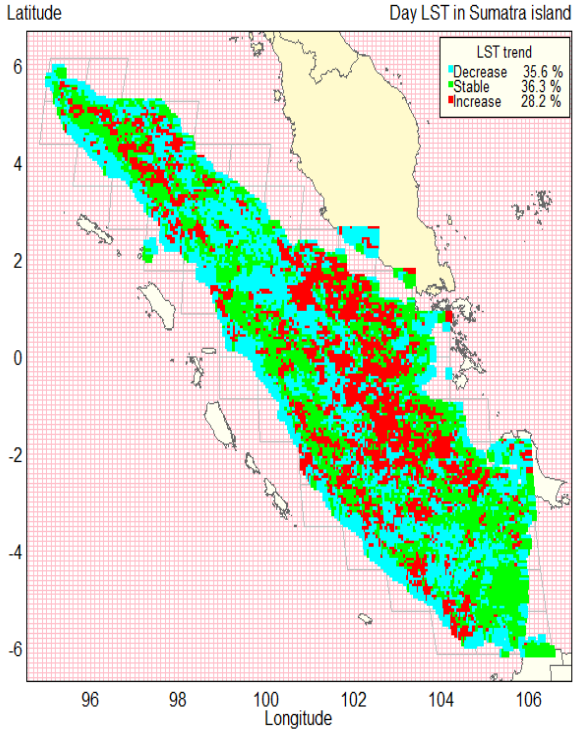

Figure 6. LST day changing trend by cubic spline model in Sumatra 2000-2018.

Figure 6 represented the LST day change based on cubic spline result which a prediction from time series data since 2000-2018. The increasing accelerations (red area) is occurred in many areas in Sumatra island and decreasing accelerations (blue area) is occurred in some areas also, and stable (Green area).

DISCUSSION

Seasonal pattern of this research showed that the highest LST-day in all area of region 25 super region 1 happened between day 229 and day 267. Other findings in of seasonal pattern in area with four season show that the highest LST appeared in summer season(21). In another region, the highest LST was emerged between May to September(22). Finding of seasonal pattern from some different area leading us that LST affected by other factor such as vegetation and land use-land cover (LULC) and surface solidity(23).

Research on Land-Use and Land-Cover Change (LUCC) using remote sensing technology has a long history and has made progress (24). LUCC is an important indicator in understanding the interactions between human activities and the environment (25). The linear change of temperature and its association with land cover depends upon many environmental factors. Land cover (i.e. urban land) has relationship with high pollution and temperature change(26). The land cover has a substantial impact on urban environmental conditions such as biodiversity, climate change, and atmosphere particulate pollution at local and/or global scales(27,28).

A study in West Sumatra depict the same result with this study that there was variation in increased of average air surface temperature (29). In other study that this variation was affecting by many factor such as elevation, normalized difference vegetation index (NDVI), and land cover (26,30,31). The great variation on land elevation has a major impact on LST (32). Other findings had presented land cover product between surface urban heat island (SUHI) and urban heat island (UHI) which were effect measured from LST maps and air temperature (AT) data (33). Vegetation correlated with most of factors which cause climate change including temperature changing. NDVI is being a tool for analyzing the vegetation status in present, past, and predict its future. According to Sharma et al. (2018), Normalized Difference Vegetation Index (NDVI) is created based on MODIS remote sensors capturing the spectral behavior of vegetation.

CONCLUSION

Little variations were exhibited by daily seasonal pattern for LST-day (˚C). LST-day was

increased in the beginning of year and decreased at the end of the year. This study finding also mentioned that not all LST in area of Sumatra island was increased. Other factors that affecting this variation must be investigated such as elevation, NDVI and land cover.

ACKNOWLEDGEMENTS

This research was supported by the Thailand's Education Hub for ASEAN Countries (TEH-AC).

REFERENCES

1. Wongsai N, Wongsai S, Huete AR. Annual seasonality extraction using the cubic spline function and decadal trend in temporal daytime MODIS LST data. Remote Sens. 2017;9(12).
2. Li ZL, Tang BH, Wu H, Ren H, Yan G, Wan Z, et al. Satellite-derived land surface temperature: Current status and perspectives. Remote Sens Environ [Internet]. 2013;131:14–37. Available from: http://dx.doi.org/10.1016/j.rse.2012.12.008.
3. Marjuki, van der Schrier G, Tank AMGK, van den Besselaar EJM, Nurhayati, Swarinoto YS. Observed trends and variability in climate indices relevant for crop yields in Southeast Asia. J Clim. 2016;29(7):2651–69.
4. Wheeler T, von Braun J. Climate Change Impacts on Global Food Security. Vol. 341, Science (New York, N.Y.). 2013. 508–513 p.
5. Alexandratos N, Bruinsma J. World agriculture towards 2030/2050: the 2012 revision. Vols. 12–03, ESA Working paper No. 12-03. Rome, FAO. 2012.
6. Me-Ead C, McNeil N. Graphical display and statistical modeling of temperature changes in tropical and subtropical zones. Songklanakarin J Sci Technol. 2016;38(6):715–21.
7. Rijal S, Saleh MB, Surati IN, Tiryana T. Deforestation Profile of Regency Level in Sumatra. Int J Sci Basic Appl Res. 2016;25(2):385–402.
8. Sharma I, Ueranantasun A, Tongkumchum P. Modeling of satellite data to identify the seasonal patterns and trends of vegetation index in Kathmandu Valley, Nepal from 2000 to 2015. J Teknol. 2018;80(4):125–33.
9. ORNL DAAC. MODIS and VIIRS Land Products Global Subsetting and Visualization Tool [Internet]. ORNL Distributed Active Archive Center; 2018. Available from: https://daac.ornl.gov/cgi-bin/dsviewer.pl?ds_id=1379.
10. Phan TN, Kappas M, Tran TP. Land Surface Temperature Variation Due to Changes in Elevation in Northwest Vietnam. Climate. 2018;6(28):1–19.
11. Wan Z. New Refinements and Validation of the MODIS Land-Surface Temperature/Emissivity Products. Vol. 140, Remote Sensing of Environment. 2008. 59–74 p.
12. Wan Z, Hook S, Hulley G. MOD11A2 MODIS/Terra Land Surface Temperature and Emissivity 8-Day L3 Global 1km SIN Grid V006. NASA EOSDIS L Process DAAC [Internet]. 2015 [cited 2019 Feb 2]; Available from: https://modis.ornl.gov/subsetdata/07Jan2019_11:57:25_749108552L28.658558L77.1221S81L81_MOD11A2/citation.bib.
13. Team RC. R: A Language and Environment for Statistical Computing [Internet]. Vol. 2009, Vienna, Austria. 2018 [cited 2019 Feb 2]. p. 1–9. Available from: https://www.r-project.org/.
14. Wold S. Spline Functions in Data Analysis. Technometrics [Internet]. 1974;16(1):1–11. Available from: http://www.jstor.org/stable/1267485.
15. Tularam GA, Ilahee M. Time series analysis of rainfall and temperature interactions in coastal catchments. J Math Stat. 2010;6(3):372–80.
16. Zhao Y, Ge L, Zhou Y, Sun Z, Zheng E, Wang X, et al. A new Seasonal Difference Space-Time Autoregressive Integrated Moving Average (SD-STARIMA) model and spatiotemporal trend prediction analysis for Hemorrhagic Fever with Renal Syndrome (HFRS). PLoS One. 2018;13(11):1–20.
17. Sharma I, Tongkumchum P, Ueranantasun A. Modeling of Land Surface Temperatures to determine temperature patterns and detect their association with altitude in the Kathmandu Valley of Nepal. Chiang Mai Univ J Nat Sci. 2018;17(4):275–88.
18. Noi PT, Kappas M, Degener J. Estimating daily maximum and minimum land air surface temperature using MODIS land surface temperature data and ground truth data in Northern Vietnam. Remote Sens. 2016;8(12):1–24.
19. Yang YZ, Cai WH, Yang J. Evaluation of MODIS land surface temperature data to

estimate near-surface air temperature in Northeast China. Remote Sens. 2017;9(5):1–19.
20. Irwandi H, Sudrajat A. Analisis tren suhu udara dan curah hujan di sumatera utara. In: Simposium VIII PERHIMPI. 2012. p. 201–12.
21. Singh RB, Grover A, Zhan J. Inter-seasonal variations of surface temperature in the urbanized environment of Delhi using landsat thermal data. Energies. 2014;7(3):1811–28.
22. Khorchani M, Martin-Hernandez N, Vicente-Serrano SM, Azorin-Molina C, Garcia M, Domínguez-Duran M[a]. A, et al. Average annual and seasonal land surface temperature, spanish peninsular. J Maps. 2018;14(2):465–75.
23. Khandelwal S, Goyal R, Kaul N, Mathew A. Assessment of land surface temperature variation due to change in elevation of area surrounding Jaipur, India. Egypt J Remote Sens Sp Sci [Internet]. 2018;21(1):87–94. Available from: https://doi.org/10.1016/j.ejrs.2017.01.005
24. Sun L, Wei J, Duan DH, Guo YM, Yang DX, Jia C, et al. Impact of Land-Use and Land-Cover Change on urban air quality in representative cities of China. J Atmos Solar-Terrestrial Phys. 2016;142(March 2019):43–54.
25. Dewan AM, Yamaguchi Y, Rahman MZ. Dynamics of land use/cover changes and the analysis of landscape fragmentation in Dhaka Metropolitan, Bangladesh. GeoJournal. 2012;77(3):315–30.
26. Sun Q, Wu Z, Tan J. The relationship between land surface temperature and land use/land cover in Guangzhou, China. Environ Earth Sci. 2012;65(6):1687–94.
27. Nagendra H, Munroe DK, Southworth J. From pattern to process: landscape fragmentation and the analysis of land use/land cover change. Agric Ecosyst Environ [Internet]. 2004;101(2):111–5. Available from: http://www.sciencedirect.com/science/article/pii/S0167880903003189.
28. Uy PD, Nakagoshi N. Analyzing urban green space pattern and eco-network in Hanoi, Vietnam. Landsc Ecol Eng. 2007;3(2):143–57.
29. Musyayyadah HA, Vonnisa M. Analisa Pola Temperatur Udara Permukaan di Sumatera Barat Tahun 1980 - 2017. J Fis Unand. 2019;8(1):91–7.
30. Guan Y, Dan Q, Zhang C, Cai D, Xuying LIU, GUO Shan 郭杉. Urban Surface Energy Distribution and Related Characteristics : An Remote Sensing Based Research Applied to the International Livable Cities. J Geo-Information Sci. 2014;16(5):806-814.
31. Alavipanah S, Wegmann M, Qureshi S, Weng Q, Koellner T, Alavipanah S, et al. The Role of Vegetation in Mitigating Urban Land Surface Temperatures: A Case Study of Munich, Germany during the Warm Season. Sustainability [Internet]. 2015;7(4):4689–706. Available from: http://www.mdpi.com/2071-1050/7/4/4689.
32. Gao M, Qin Z, Qiu J, Liu S, Xu B, Li W, et al. Retrieving spatial-temporal variation of land surface temperature in Tibetan Plateau for the years 2005-2006 from MODIS satellite data. 2008;7110(June 2014):71101A-71101A–10.Availablefrom: http://proceedings.spiedigitallibrary.org/proceeding.aspx?articleid=1328574.
33. Sobrino JA, Oltra-carrió R, Sòria G, Jiménez-muñoz JC, Franch B, Hidalgo V, et al. Evaluation of the surface urban heat island effect in the city of Madrid. Int J Remote Sens. 2013;34(9):3177–92.

****